Supplementary information for

A decomposition of the atmospheric and surface contributions to the outgoing longwave radiation

Han Huang, Yi Huang

Department of Atmospheric and Oceanic Sciences, McGill University, Montreal, Canada

Corresponding Author: Han Huang, han.huang2@mcgill.ca (ORCID: 0000-0002-9143-6453)

Band	Wavenumber (cm^{-1})	Number of g-points	Influential gases
1	10 - 350	10	H_2O, N_2
2	350 - 500	12	H_2O
3	500 - 630	16	H_2O, CO_2, N_2O
4	630 - 700	14	H_2O, CO_2, O_3
5	700 - 820	16	H_2O, CO_2, O_3, CCl_4
6	820 - 980	8	H_2O, CO_2, CFC_{11}, CFC_{12}
7	980 - 1080	12	H_2O, O_3, CO_2
8	1080 - 1180	8	H_2O, CO_2, O_3, N_2O, CFC_{12}, CFC_{22}
9	1180 - 1390	12	H_2O, CH_4, N_2O
10	1390 - 1480	6	H_2O
11	1480 - 1800	8	H_2O, O_2
12	1800 - 2080	8	H_2O, CO_2
13	2080 - 2250	4	H_2O, N_2O, CO_2, CO, O_3
14	2250 - 2380	2	CO_2
15	2380 - 2600	2	N_2O, CO_2, H_2O, N_2,
16	2600 - 3250	2	H_2O, CH_4

Table 1. RRTMG bands and influential gases (from RRTMG LW instructions, http://rtweb.aer.com/rrtm_frame.html).

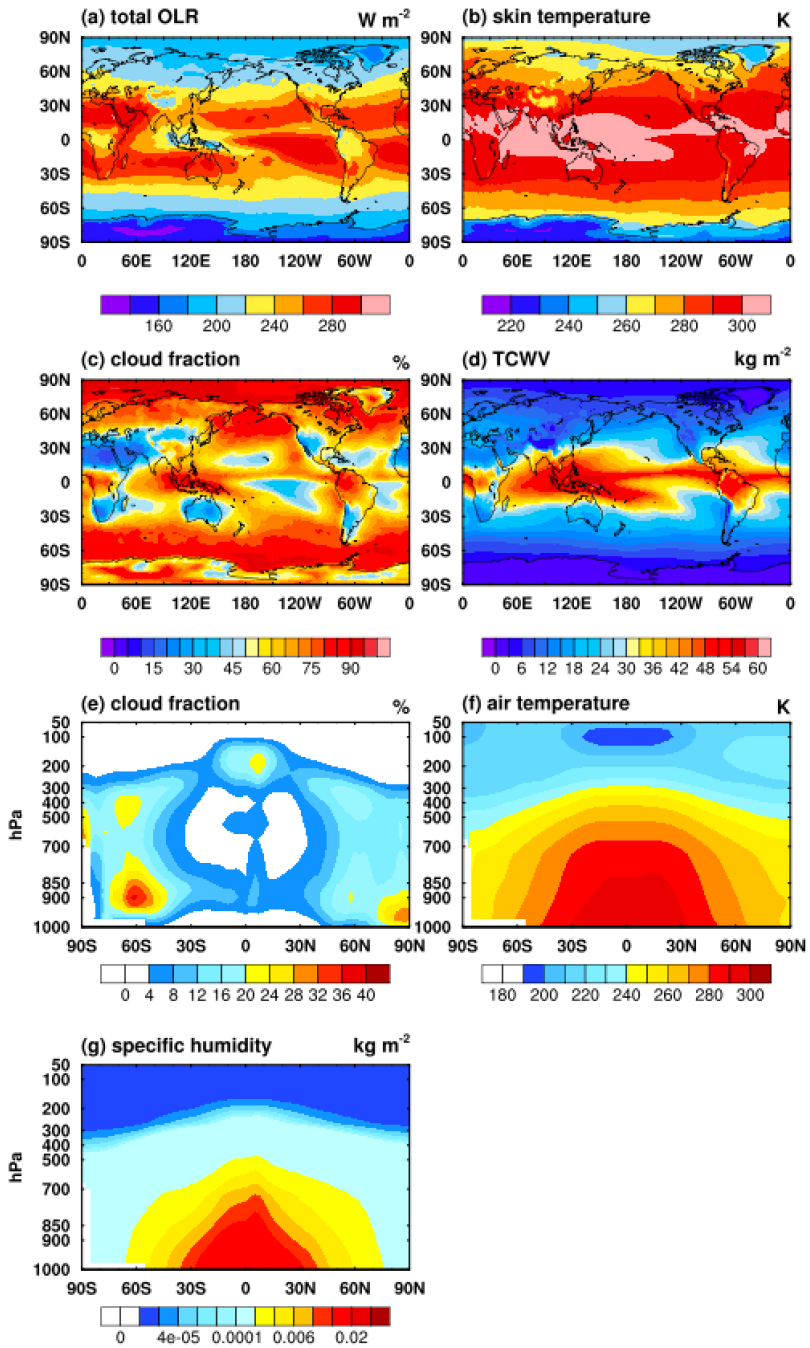

Figure S1. Annual mean (a) total OLR, units: W m^{-2}, (b) skin temperature, units: K, (c) cloud fraction, units: %, (d) total column water vapor (TCWV), units: kg m^{-2}, (e) zonal mean vertical distribution of cloud fraction, units: %, (f) zonal mean vertical distribution of air temperature, units: K, (g) zonal mean vertical distribution of specific humidity, units: kg m^{-2}, in 2013 of ERA5. The global mean values of total OLR and skin temperature in 2013 are 242.03 W m^{-2} and 288.36 K, respectively. In comparison, the multi-year (2013 to 2018) average (as well as the interannual standard deviation) of total OLR and skin temperature are 242.15 W m^{-2} (0.14 W m^{-2}) and 288.54 K (0.14 K), which shows that 2013 is a "normal" year.

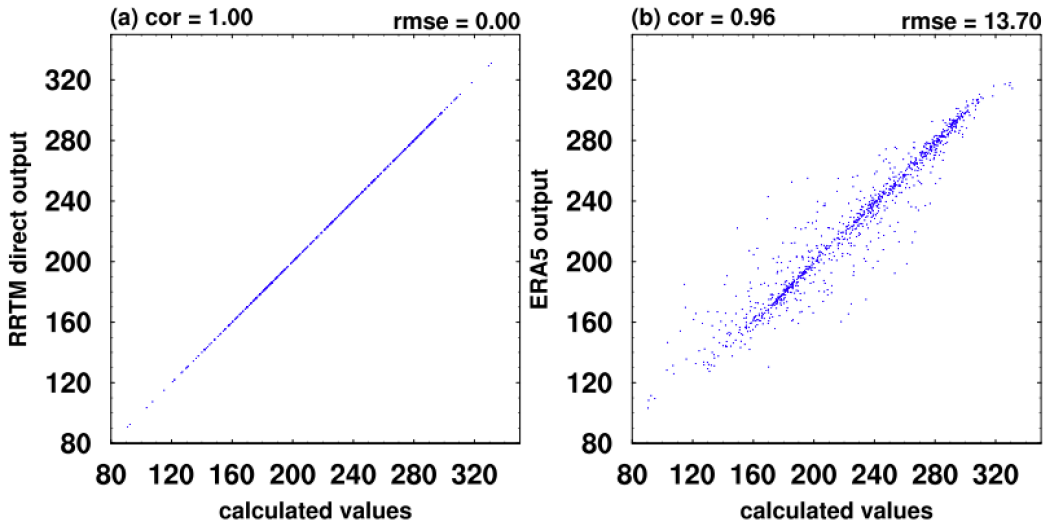

Figure S2. Validations of total OLR over the whole globe in all sky between (a) calculated values using Equation 1 and direct output from RRTMG, (b) RRTKG-simulated results and direct output from ERA5 at one time slice, units: W m^{-2}. cor is the correlation between two series and $rmse$ is the root-mean-square-error. The results here confirm the validity of both the decomposition method described in Section 2.1 and the RRTMG simulations.

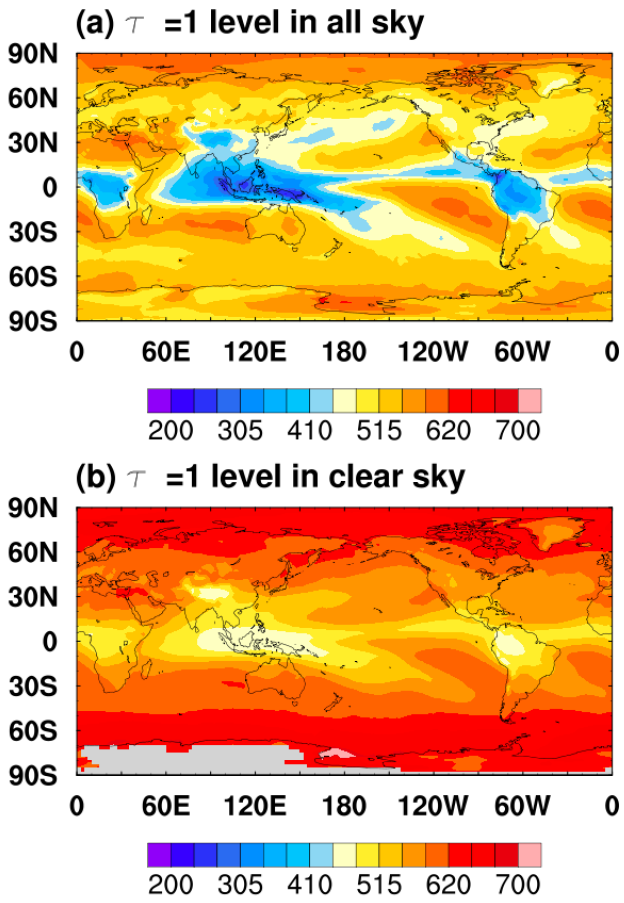

Figure S3. Annual mean pressure of the τ=1 level in (a) all sky, and (b) clear sky. The plots are based on the broadband optical depth values derived using Equation (8). The missing value (grey region in (b)) indicates the total atmospheric optical depth is smaller than 1.

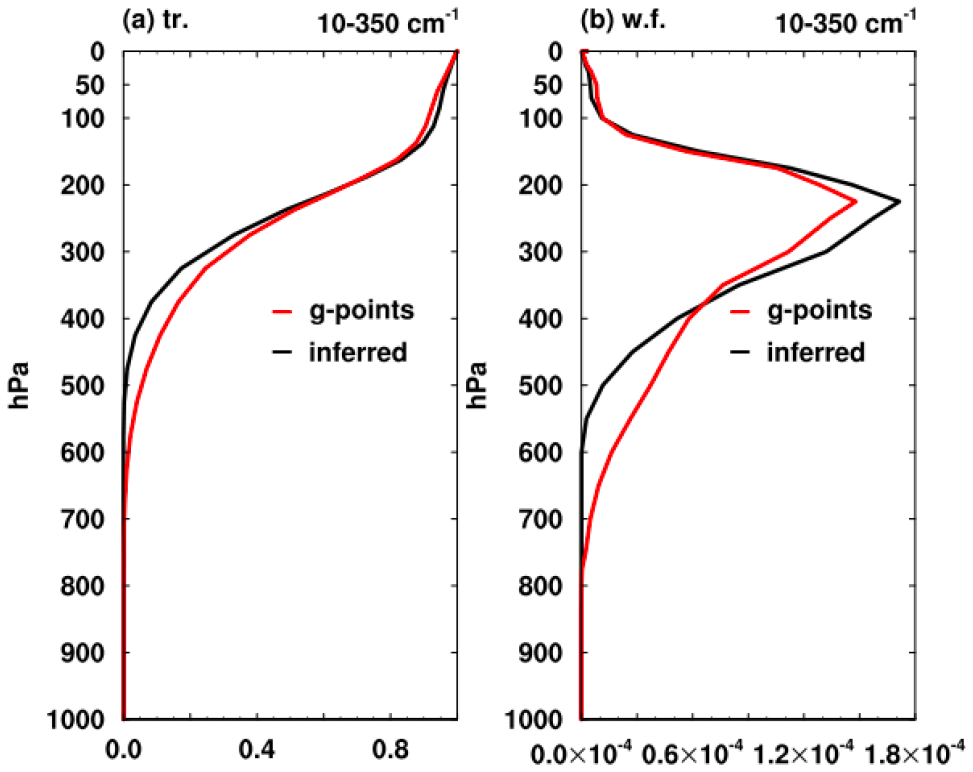

Figure S4. Comparison of (a) transmittance and (b) weighting functions between the inferred method (Equation (4)) and the averaged values from the g-points in the 10-350 cm^{-1} band at a random location (15N, 100E) in clear-sky.

Here we provide more descriptions of the inference method for the atmospheric transmission and derived weighting functions. Based on Equation (6) and (7), the inferred transmittance of a layer can be written as:

$$\Delta\widetilde{tr}_i = \frac{F_i^{down} - F_{i+1}^{up}}{F_{i+1}^{down} - F_i^{up}} \quad (S1)$$

Here $\Delta\widetilde{tr}_i$ is the inferred transmittance in the i^{th} layer and hence the transmittance between the the i^{th} layer and the TOA is $\widetilde{tr}_i = \prod_1^i \Delta\widetilde{tr}_j$. In theory, the transmittance at any given level should be positive and no bigger than unity. However, the derived transmittance based on Equation (S1) may violate the physical expectation due to anomalous flux profiles. We find that negative transmittance may occur when the optical depth is very high, e.g., in strong absorption bands, which decouples the incident and transmitted radiance in either upward or downward direction. To fix this, we correct the inferred transmittance value to 0. Inferred transmittance greater than 1 occurs less frequently and usually happens when there is a temperature inversion. In this circumstance, we set the inferred value to 1 and the corresponding optical depth in that layer to a representative value of 10^{-4}. All results in this work are corrected using this method.

As mentioned in the main text, the choice of vertical coordinate affects the shape of weighting function, here we further show a comparison of weighting functions defined as $\frac{dtr}{dp}$ and $\frac{dtr}{dz}$ after the corrections mentioned above in Figure S5.

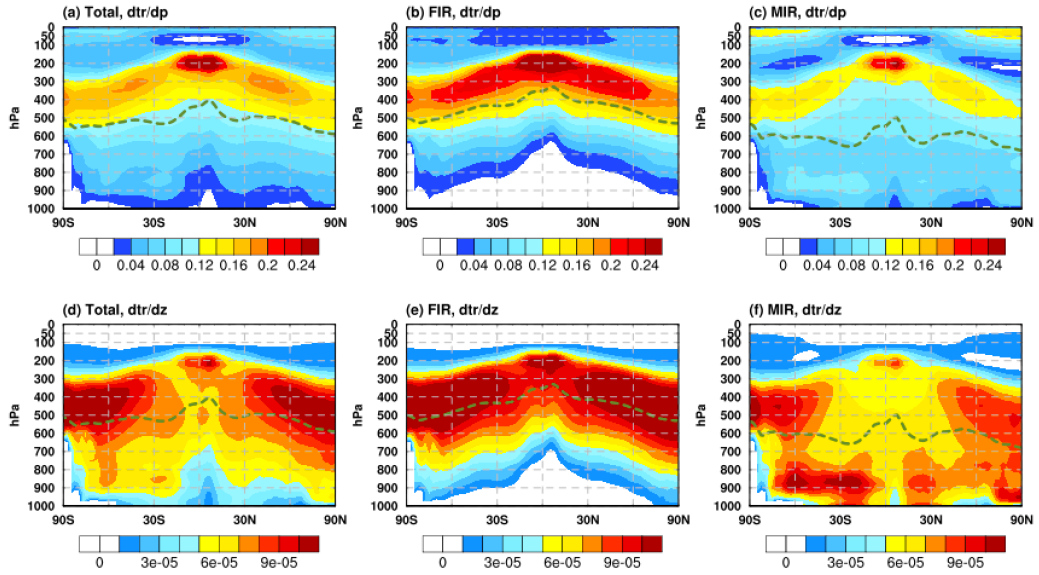

Figure S5. Annual mean derived weighting function in all sky defined as (a, b, c) $\frac{dtr}{dp}$ and (d, e, f) $\frac{dtr}{dz}$. The dashed dark green line is the inferred $\tau = 1$ level. The difference between the $\frac{dtr}{dp}$ and $\frac{dtr}{dz}$ comes from the density (ρ) effect ($\frac{dp}{dz} = -\rho g$), which takes larger values and thus suppresses the value of $\frac{dtr}{dp}$ in the lower layers. In comparison, we see $\frac{dtr}{dz}$ better corresponds to the location of cloud layers (e.g., Figure S5f). Moreover, as expected, the level of maximum values of $\frac{dtr}{dz}$ (panels d-f) better corresponds with the $\tau = 1$ level.

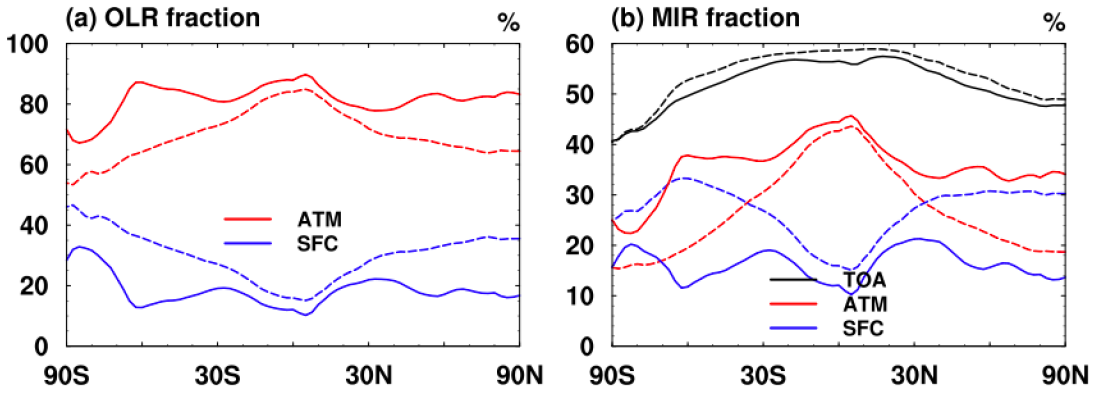

Figure S6. Annual mean (a) atmospheric and surface fractional contribution to the total OLR at the TOA, units: %. (b) zonal mean MIR fraction with respect to local total OLR, decomposed into contributions from the atmosphere and surface, units: %. Solid lines represent the results in all sky and dash lines in clear sky.

In total OLR, the atmosphere makes a major contribution to total OLR (panel a) at each latitude. The MIR fraction at the TOA decreases from the tropics at 60% to about 40% at the poles. The variation of the atmospheric and surface contribution with latitudes are opposite in both total OLR and MIR, as the decrease of water vapor concentration with latitudes weakens the local emission in the atmosphere and allows more surface emission to reach the TOA.

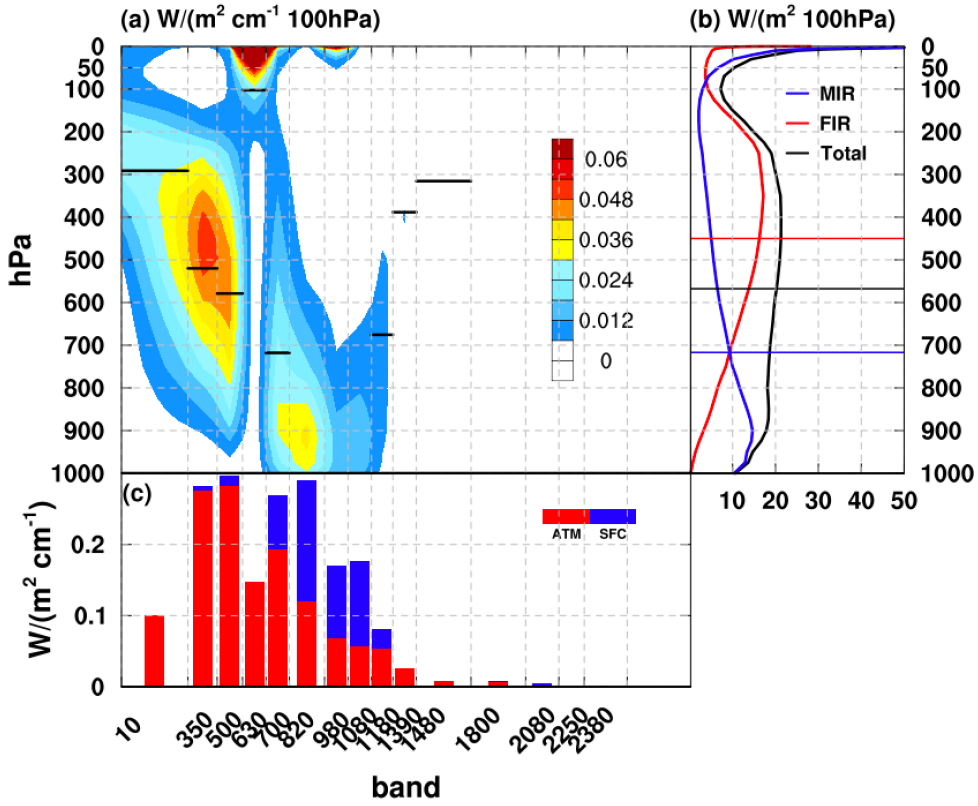

Figure S7. Clear-sky global annual mean spectral and vertical decomposition of OLR. (a) Layer-wise atmospheric contribution to the OLR irradiance flux in each of the 16 RRTMG bands, units: W/(m^2 cm^{-1} 100hPa). (b) Spectrally integrated layer-wise contribution, units: W/(m^2 100hPa). (c) Vertical integrated atmospheric contribution, in comparison with the surface contribution, units: W/(m^2 cm^{-1}). The horizontal lines in (a) and (b) are the inferred τ=1 level using the diagnostic method described in Section 2.

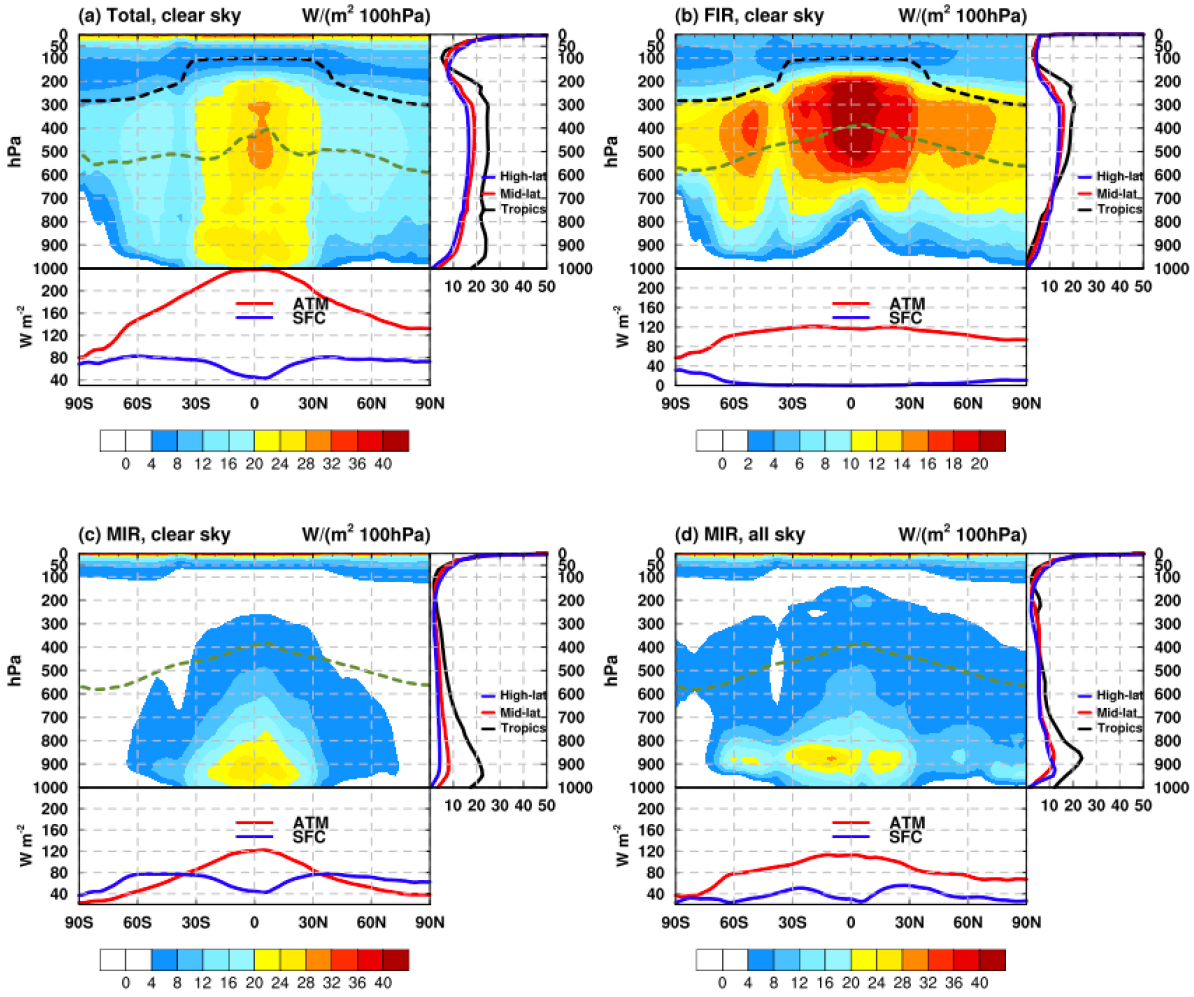

Figure S8. Same as Figure 4, but for the annual and zonal mean OLR fluxes in (a) total OLR, (b) FIR, (c) MIR in clear sky, and (d) MIR in all sky.

The vertical distribution in clear sky is more uniform in total OLR, compared with results in all sky. Different from FIR, the atmospheric contribution in MIR is maximized at the lower atmosphere. In both total OLR and MIR in clear sky, the surface contribution shows a local minimum in the tropics due to the high water vapor concentration and shows little variation in the extratropics. The relatively weaker surface contribution in southern polar region in MIR in clear sky is due to the local lower surface temperature.

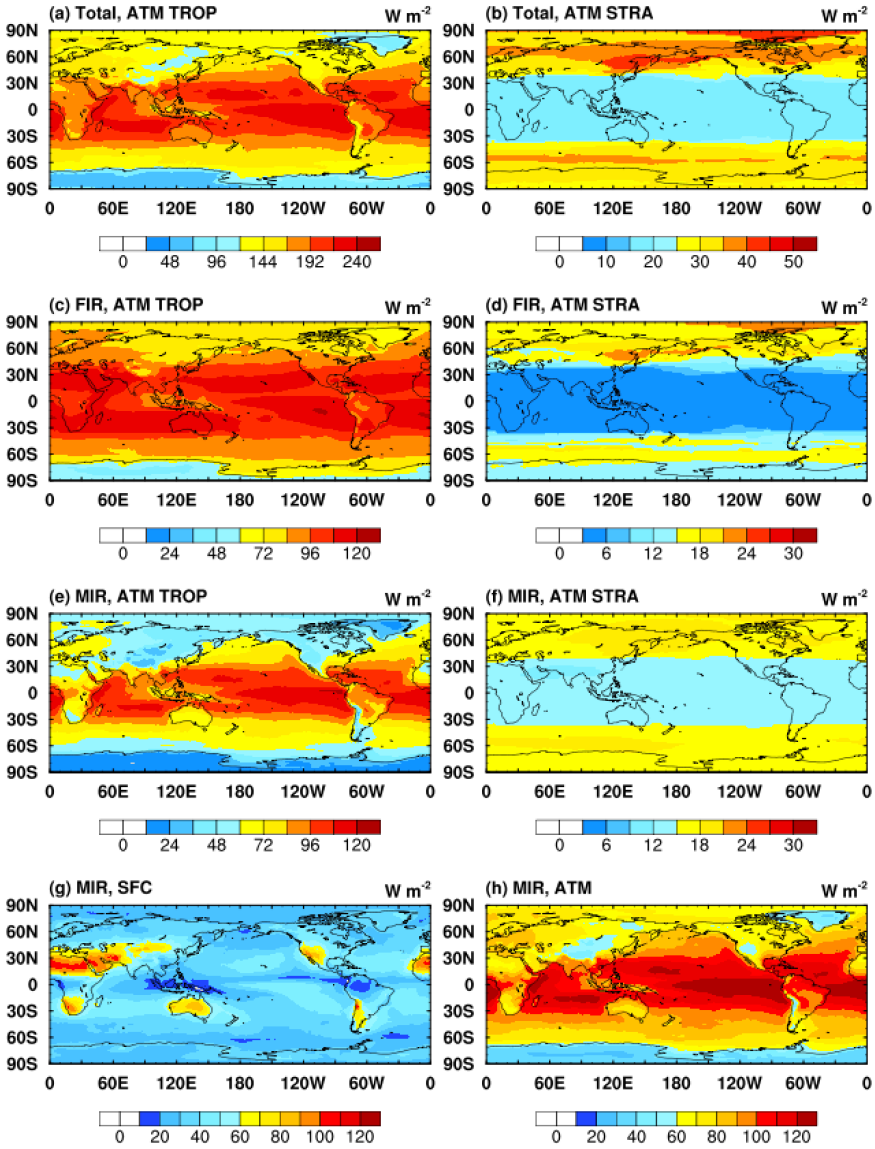

Figure S9. (a-f) Annual mean tropospheric and stratospheric contributions to the total OLR, FIR and MIR in all sky, (g) annual mean surface contribution in MIR, (h) annual mean total column atmospheric contribution in MIR (the sum of (e) and (f)). The troposphere and stratosphere are divided based on the tropopause in Figure 4.

The total OLR and MIR in the troposphere show noticeable gradients from the equator to the poles while FIR is more uniform. All the three plots (Figure S9 a, c, e) show a local minimum contribution in the ITCZ region. In the stratosphere, the contribution is much more uniform than in the troposphere, with a clear contrast between the tropics and extratropics; the weaker contributions in the tropics are due to higher tropopause and lower stratospheric temperature.

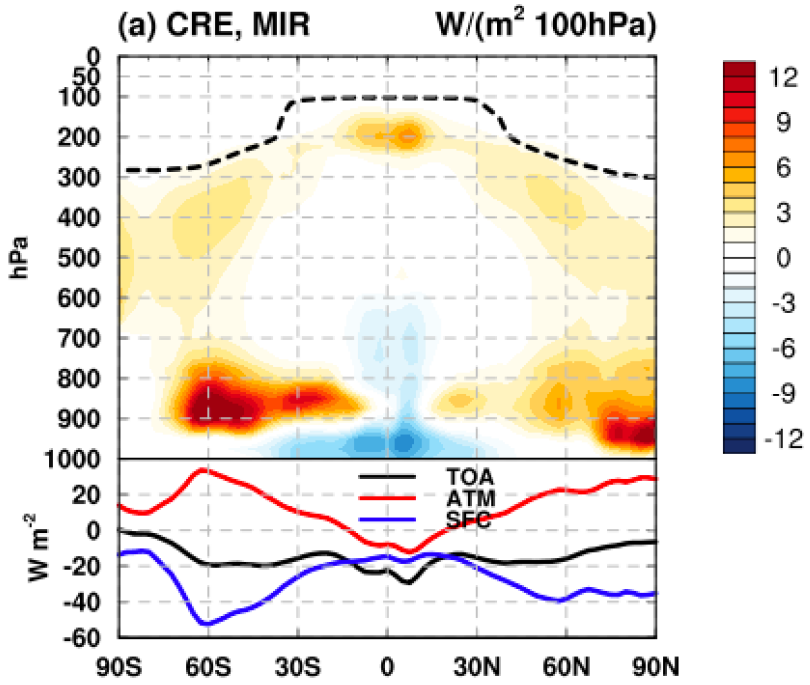

Figure S10. Annual mean and zonal mean cloud radiative effect intensity in MIR, units: W/(m^2 100hPa). Line plots show the vertically integrated atmospheric contribution and surface contribution, units: W m^{-2}. The black dash line in contour plots represents the tropopause.

The CRE in MIR in the tropics comes from both the reduction of transmission in the lower atmosphere and the increase of emission at about 200hPa, while in the extratropics, it is more from the enhanced emission at the cloud layers (e.g., 900hPa in the southern mid-latitude).

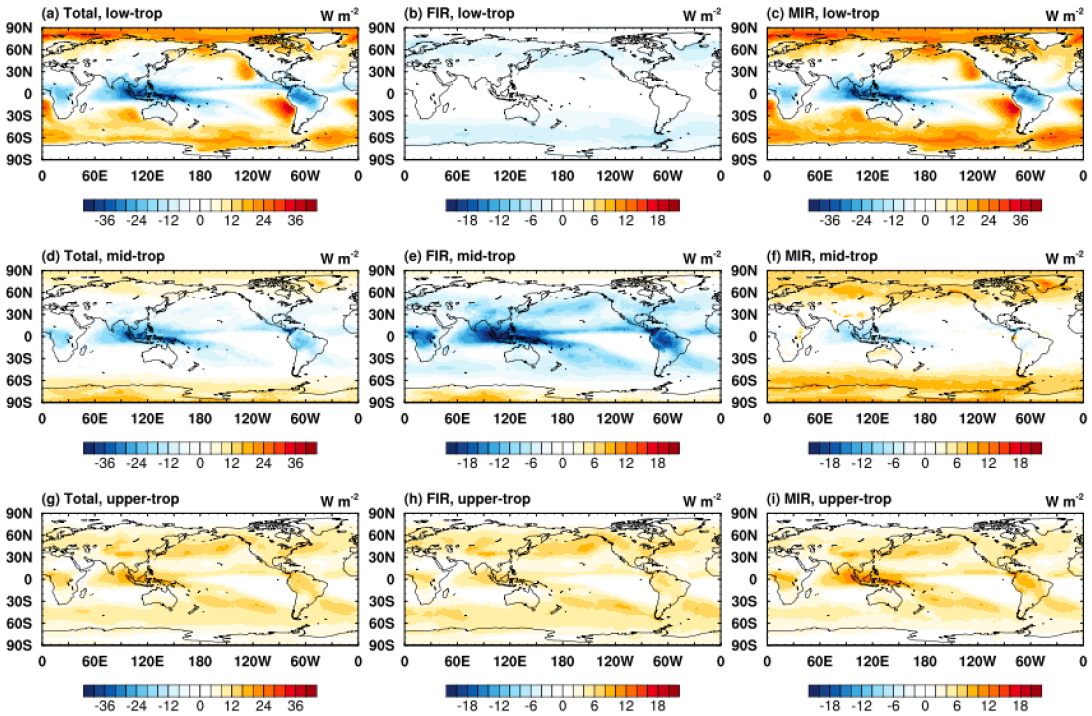

Figure S11. Annual mean cloud radiative effect in the atmosphere of different layers, units: W m^{-2}. Low-trop represents contribution from 1000hPa to 700hPa and mid-trop of 700hPa-400hPa, upper-trop of 400hPa -100hPa.

In the lower-troposphere (first row), CRE is negative in the tropics and positive in the extratropics with regard to the total OLR (panel a), which largely results from the cloud effect in MIR (panel b), where high clouds reduce the atmospheric transmission from this level (lower-troposphere) to TOA in the tropics and low clouds enhance atmospheric emissivity and thus lower-tropospheric contribution to OLR in the extratropics; in contrast, in FIR, due to the strong water vapor absorption, the OLR is insensitive to clouds and the CRE is negligible in the tropics. In the mid-troposphere (second row), the dampened transmission due to higher clouds affects both the total OLR and FIR, while in MIR the change in the tropics is weak and CRE is noticeably more in the mid-to-high latitudes. In the upper-troposphere (third row), the atmospheric contributions all increases due to the increase of atmospheric emissivity caused by the clouds.

W m^{-2}	all sky		clear sky		CRE (all sky – clear sky)	
	total	FIR	total	FIR	total	FIR
Lower-trop	66.39	18.51	65.80	20.72	0.59	-2.21
Mid-trop	63.75	43.67	67.31	49.07	-3.57	-5.40
Upper-trop	55.04	42.41	46.95	38.39	8.08	4.02
Strato	16.18	4.13	16.18	4.13	0.00	0.00

Table S2. Annual mean and global mean atmospheric contributions in different layers. The cloud radiative effect (CRE) is the difference between the all-sky and clear-sky values, units: W m^{-2}. Lower-troposphere represents contribution from surface (~1000hPa) to 700hPa, mid-troposphere from 700hPa to 400hPa, upper-troposphere from 400hPa to100hPa, and stratosphere from 100hPa to TOA. Note that here the definition of stratosphere is different from that in Table 1 The difference between the values roughly measures the contribution in the extratropical lower-most stratosphere (between the tropopause and the 100hPa level).